Numerical investigation of unsteady cavitation around a NACA 66 hydrofoil using OpenFOAM

2014 IOP Conf. Ser.: Earth Environ. Sci. 22 052013

(http://iopscience.iop.org/1755-1315/22/5/052013)

IOP Conf. Series: Earth and Environmental Science **22** (2013) 052013 doi:10.1088/1755-1315/22/5/052013

Numerical investigation of unsteady cavitation around a NACA 66 hydrofoil using OpenFOAM

V. H. Hidalgo[1,3], X. W. Luo[1*], X. Escaler[2], J. Ji[1] and A. Aguinaga[3]

[1] State Key Laboratory of Hydro Science & Engineering, Tsinghua University, Beijing, China
[2] Centre for Industrial Diagnostics and Fluid Dynamics, UPC, Barcelona, Spain
[3] Department of Mechanical Engineering, Escuela Politecnica Nacional, Quito, Ecuador

E-mail: luoxw@mail.tsinghua.edu.cn

Abstract. The prediction and control of cavitation damage in pumps, propellers, hydro turbines and fluid machinery in general is necessary during the design stage. The present paper deals with a numerical investigation of unsteady cloud cavitation around a NACA 66 hydrofoil. The current study is focused on understanding the dynamic pressures generated during the cavity collapses as a fundamental characteristic in cavitation erosion. A 2D and 3D unsteady flow simulation has been carried out using OpenFOAM. Then, Paraview and Python programming language have been used to characterize dynamic pressure field. Adapted Large Eddy Simulation (LES) and Zwart cavitation model have been implemented to improve the analysis of cloud motion and to visualize the bubble expansions. Additional results also confirm the correlation between cavity formation and generated pressures.

1. Introduction

Unsteady cavitation produces undesirable effects in hydraulic installations as hydropower turbines, pumps or naval propellers [1]. In Francis turbines, the unsteady cavitating flow is associated with noise and vibration, that may induce cyclic stresses and damage to material surface, and the degradation of performance [2]. Inlet cavitation occurs when the pressure decreases to saturation vapor pressure on the turbine blade suction side [2]. The unsteadiness of the inlet cavitation is associated with the generation of bubble clouds that collapse near the blade surface and produce damage. Therefore, studies of leading edge cavitation around hydrofoils are important to understand this phenomenon.

The premise of homogeneous flow for numerical study of cavitation was presented by Kubota et al. [3]. The so-called bubble two phase flow, BTF, is based on Rayleigh-Plesset equation and it neglects the effects of surface tension and viscous damping. Coutier-Delgosha et al. [4] carried out a simulation in a venturi-type duct to understand cavity shedding based on the premise of homogeneous flow, where the condensation and vaporization are controlled by barotropic state law. Other studies were presented based on volume fraction of vapor or liquid and mass transport for condensation and evaporation [5–7]. Therefore, these ideas are the basis of the present research.

The traditional method in Computational Fluid Dynamics (CFD) is Reynolds Average Navier Stockes (RANS) that is used to solve a wide range of problems in the aerospace and naval industry [8]. However, for unsteady cavitating flows at high Reynolds numbers, RANS needs

to be adapted [9–12]. The numerical results obtained by Ji et al. [13] in their study "Three-dimensional Large Eddy Simulation (LES) and vorticity analysis of unsteady cavitating flow around a twisted hydrofoil" show good accuracy with experiments. Therefore, LES has been proved to be a good option for numerical simulation of cavitating flows, and, consequently, this model is used in the present study.

The challenge of the current work is not only to study 2D and 3D cavitation on NACA 66 hydrofoil, but also to validate the use of Free/Open Source Software (FOSS). In particular, programs and programming languages as Salome, OpenFOAM, python and C++ have been used for the numerical simulation. The FOSS advantage is the possibility to change the main code for our needs.

2. Physical description

The vapor volume fraction α is used to find the fluid density ρ and dynamic viscosity μ, as shown in eq. (1) to eq. (3).

$$\alpha = \frac{\forall_{\mathrm{V}}}{\forall} \tag{1}$$

$$\rho = (1-\alpha)\rho_{\mathrm{L}} + \alpha\rho_{\mathrm{V}} \tag{2}$$

$$\mu = (1-\alpha)\mu_{\mathrm{L}} + \alpha\mu_{\mathrm{V}} \tag{3}$$

where $\forall$ is the total volume, L and V are the subindex for liquid and vapor respectively.

2.1. Mathematical Considerations

Continuity and Navier Stokes equations are used to describe and solve the cavitation phenomenon. Favre-filtering operation is part of LES model, so it is applied to these equations, which is denoted by an over bar in the variables, as observed in eq. (4) to eq. (6).

$$\frac{\partial \overline{u}_j}{\partial x_j} = \dot{m}\left(\frac{1}{\rho_{\mathrm{L}}} - \frac{1}{\rho_{\mathrm{V}}}\right) \tag{4}$$

$$\frac{\partial(\alpha)}{\partial t} + \frac{\partial(\alpha\overline{u}_j)}{\partial x_j} = \frac{\dot{m}}{\rho_{\mathrm{V}}} \tag{5}$$

$$\frac{\partial(\rho\overline{u}_i)}{\partial t} + \frac{\partial(\rho\overline{u}_i\overline{u}_j)}{\partial x_j} = -\frac{\partial\overline{p}}{\partial x_i} + \frac{\partial}{\partial x_j}\left[\rho\left(R_a - G\right)\right] \tag{6}$$

where u is velocity, x is variable of space, p is pressure, t is time, $\dot{m}$ is mass rate, i and j are the indexes of axes 1, 2 or 3, G is the subgrid stress tensor $(\overline{u_i u_j} - \overline{u}_i\overline{u}_j)$, and R_a is the filtered viscous stress tensor $2\nu\overline{S}_{ij}$, where ν is the kinematic viscosity and $\overline{S}_{ij}$ is the stress tensor rate $\frac{1}{2}\left(\frac{\partial\overline{u}_i}{\partial x_j} + \frac{\partial\overline{u}_j}{\partial x_i}\right)$.

3. Cavitation Models

Two cavitation models based on the Rayleigh-Plesset equation have been applied, whose differences are focused in the condensation and vaporization process [14, 15].

3.1. Schnerr-Sauer Model
Schnerr-Sauer model as shown in eq. (7) is inside of OpenFOAM as a native model, so it is not necessary to change the main code.

$$\dot{m} = \begin{cases} \dot{m}^+ = C_{\mathrm{V}} \dfrac{\rho_{\mathrm{V}} \rho_{\mathrm{L}}}{\rho} \alpha(1-\alpha) \dfrac{3}{R} \sqrt{\dfrac{2(p_{\mathrm{V}} - p)}{3\rho_{\mathrm{L}}}} & if \quad p < p_{\mathrm{V}} \\ \dot{m}^- = C_{\mathrm{C}} \dfrac{\rho_{\mathrm{V}} \rho_{\mathrm{L}}}{\rho} \alpha(1-\alpha) \dfrac{3}{R} \sqrt{\dfrac{2(p - p_{\mathrm{V}})}{3\rho_{\mathrm{L}}}} & if \quad p > p_{\mathrm{V}} \end{cases} \tag{7}$$

where C_{V} and C_{C} are empirical coefficients for condensation and vaporization [10], with values 2 and 1 respectively. Note that R is the radius of bubble and it is calculated by eq. (8), where n is the number of bubbles per unit of volume.

$$R = \sqrt[3]{\frac{\alpha}{\frac{4}{3}\pi n(1-\alpha)}} \tag{8}$$

3.2. Zwart
This cavitation model as shown in eq. (9) is not native in OpenFOAM, therefore it must be written in C++ language and implemented in OpenFOAM solvers.

$$\dot{m} = \begin{cases} \dot{m}^+ = -F_{\mathrm{V}} \dfrac{3 r_{\mathrm{nuc}}(1-\alpha)\rho_{\mathrm{V}}}{R_{\mathrm{B}}} \sqrt{\dfrac{2}{3} \dfrac{p_{\mathrm{V}} - p}{\rho_{\mathrm{L}}}} & if \quad p < p_{\mathrm{V}} \\ \dot{m}^- = F_{\mathrm{C}} \dfrac{3\alpha\rho_{\mathrm{V}}}{R_{\mathrm{B}}} \sqrt{\dfrac{2}{3} \dfrac{p - p_{\mathrm{V}}}{\rho_{\mathrm{L}}}} & if \quad p > p_{\mathrm{V}} \end{cases} \tag{9}$$

where $F_{\mathrm{V}} = 300$ and $F_{\mathrm{C}} = 0.03$ are the selected calibration constants for vaporization and condensation, $r_{\mathrm{nuc}} = 5.0 \times 10^{-6}$ is the nucleation site volume fraction and $R_{\mathrm{B}} = 1.9 \times 10^{-}6\ m$ is the typical bubble size in water [15].

Equation (9) indicates that the change of phase is not a symmetrical process, because vaporisation m^+ dependents on $(1-\alpha)$ and r_{nuc}, but condensation m^- dependents on α [14].

4. Computation Domain and Meshing

4.1. Hydrofoil
The hydrofoil NACA 66 and the computation domain are outlined in Fig. 1. The distance c corresponding to $\overline{AB}$ is the chord length of 0.15 m and the angle of attack $\widehat{BOD}$ is 6 °.

4.2. Meshing
A structured mesh has been created considering C meshing around the hydrofoil and scale distribution of elements with the FOSS Salome as shown in Fig. 2.

The number of mesh elements is indicated in Table 1. It is noted that the number of elements is similar to the number of nodes, which is a special characteristic for this structured mesh. Yplus number, y^+, is used to know the match between mesh size and LES requirements, where u_τ is the friction velocity at the nearest wall, y is the distance to the wall and ν is the kinematic viscosity, as shown in eq. (10).

$$y^+ = \frac{u_\tau y}{\nu} \tag{10}$$

The y^+ for the hydrofoil wall is between 0.15 and 4.15 in this research, thus satisfying LES requirements.

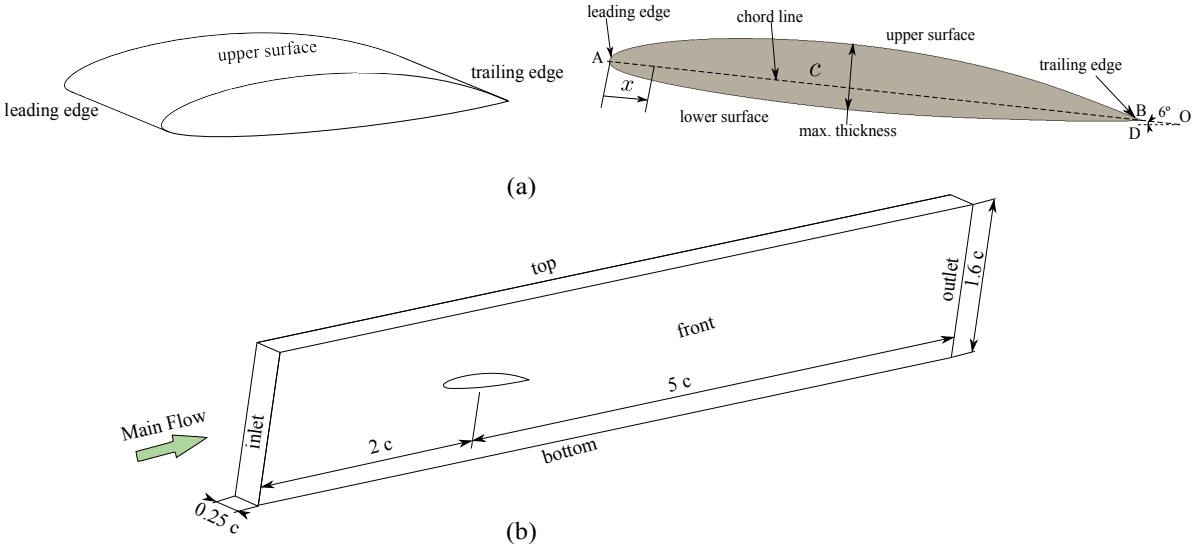

Figure 1. (a) Hydrofoil geometry and (b) Computation Domain.

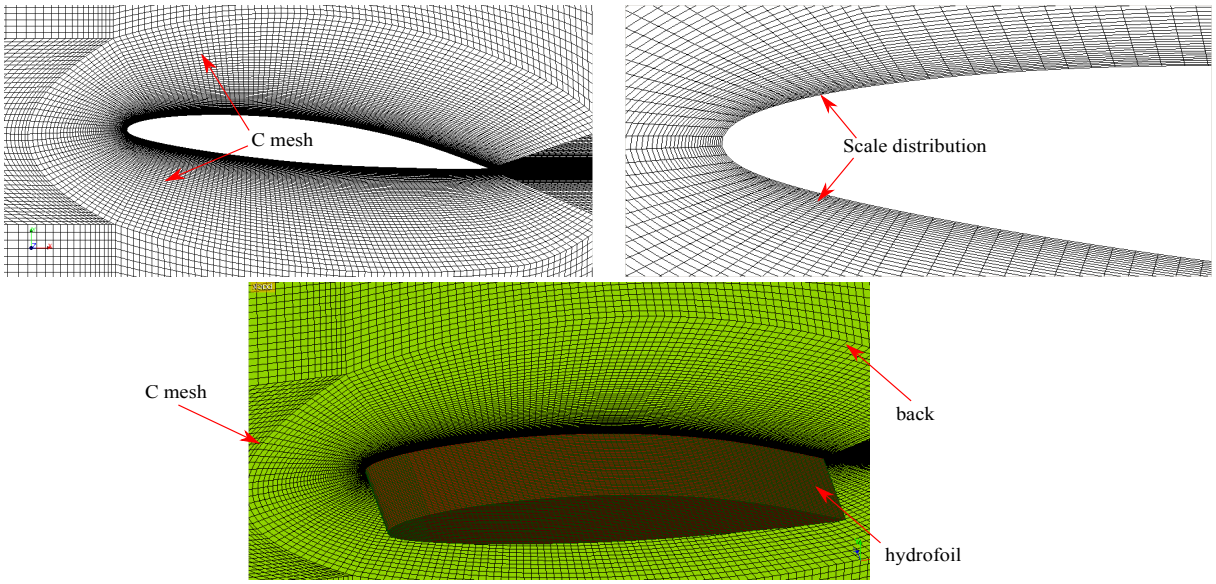

Figure 2. Structured Mesh.

5. Solver

5.1. OpenFOAM

The OpenFOAM official versions are available for the following GNU/Linux OS distributions, Ubuntu versions 12.04 to 13.10, SuSE version 12.3 and Red Hat Enterprise Linux 6.5 [16]. However, the Tsinghua university OS server runs a previous version of Red Hat 6.5, so that, an adapted version for CentOS is used that is OpenFOAM 2.2x.

The CentOS linux is based on the official distribution of Red Hat [17]. As a result, the OpenFOAM 2.2x shows like a native program in the Tsinghua university server.

Table 1. NACA 66 - STRUCTURED MESH.

Object	Mesh
Nodes	1263415
Quadrangles	127000
Hexahedrons	1216000
Elements (Total)	1347110

The Zwart model is implemented and compiled to get a new solver called vInterPhaseChangeFoam based on Anderson et al. [18]. The especial part in this research for this new solver is writing the line phaseChangeTwoPhaseMixtures/Zwart/Zwart.C in the directory vInterPhaseChangeFoam/make/files to transform Zwart as a native cavitation model in OpenFOAM.

5.2. Boundary and Operation Conditions
The numerical simulation starts at 0 s and lasts 1.5×10^{-1} s with time steps of 1×10^{-5} s. The results are saved every 25 steps. The boundary conditions are described in Table 2.

Table 2. Boundary Conditions.

Hydrofoil	Condition
Inlet	velocity in x axis $U_\infty = 5.48$ m/s
Outlet	pressure $p = p_\mathrm{r} = 20.3$ kPa
Top and Bottom	wall
Front and Back	symmetry planes
Hydrofoil wall	wall

The cavitation number is calculated by eq. (11) to know the conditions of the unsteady cavitating flow, where p_r is the absolute pressure of system and p_V is the vapor pressure equal to 2.3 kPa at 293 K. The cavitation number is 1.2, which is a similar value to the one of a previous research [1].

$$\sigma = \frac{p_\mathrm{r} - p_\mathrm{V}}{\frac{1}{2}\rho U_\infty^2} \tag{11}$$

6. Results and Discussion
The cavitation conditions at different instants of time during the periodic process of cloud detachment are shown in the rows of Fig. 3 for the experiment (central column) and both simulations. Results at analogous dimensionless time instants are presented in the same row. The coefficient ξ has been calculated with eq. 12, where the initial time is t_o and the final time is t_f. The reason for that has been the different periods of the cycle for Leroux experimental results (LE), and numerical results for Schnerr-Sauer model (SM) and Zwart model (ZM).

$$\xi = \frac{t - t_o}{t_f - t_o} \tag{12}$$

The following observations at each dimensionless time instants are found:

(i) A short cavitation sheet exits in the leading edge of the upper hydrofoil surface.

(ii) The attached sheet cavity grows along the chord .
(iii) The re-entrant jet is observed at the small dark parts in the cavity.
(iv) The sheet cavity is cut off probably by the influence of re-entrant jet, and a cloud is generated.

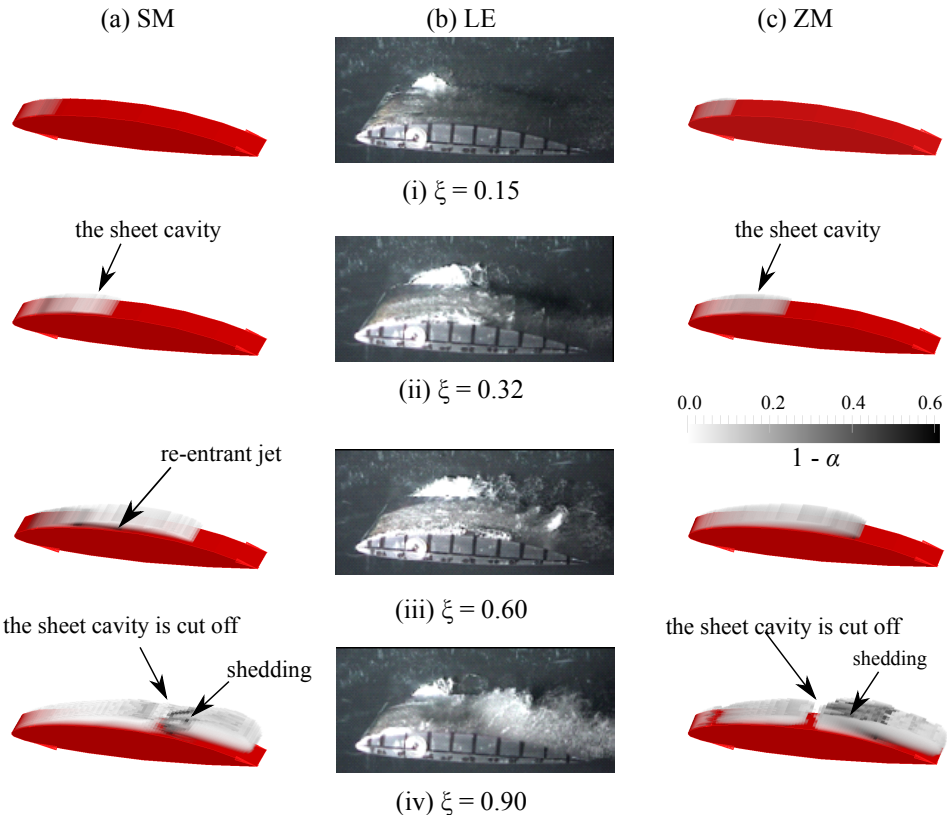

Figure 3. Cycle analysis among (a) SM, (b) EL and (c) ZM.

The SM shows similar results to ZM and EL before $\xi = 0.9$, but when the sheet cavity is cut off the SM shows smaller clouds than ZM, as observed in Fig. 3 point (iv).

The pressure fluctuation at position $x/c = 0,4$ of LE is compared with the numerical simulation results of SM and ZM. The following features can be concluded looking at Fig. 4:

1. According to LE, there is a zone of pulses between 10 and 28 kPA from $\xi = 0.03$ to $\xi = 0.30$. In the interval $\xi = 0.31 \sim 0.82$ the pressure decreases to vapor saturation pressure, and a change of phase from liquid to vapor occurs. The two pressure peaks detected at $\xi = 0.85$ and $\xi = 0.95$ might be due to the cavity cut off process.
2. In general terms, SM and ZM present outcomes similar to LE for pressure fluctuation. Looking at SM, the first pulse matches the pressure peak of 23.0 kPa at $\xi = 0.04$, then SM shows two peaks similar to LE at $\xi = 0.71$ and 0.76. However, ZM shows peaks of greater amplitude than SM and LM in the interval $0.045 < \xi < 0.090$.

In Fig. 5 2D and 3D results with the SM are compared. The 2D plane is located at 0.125 c in span-wise direction, the color scale plots represent the void fraction. Though the configuration of hydrofoil is for 2D [19], it is observed that a small part of 3D cavitation cloud with dark color

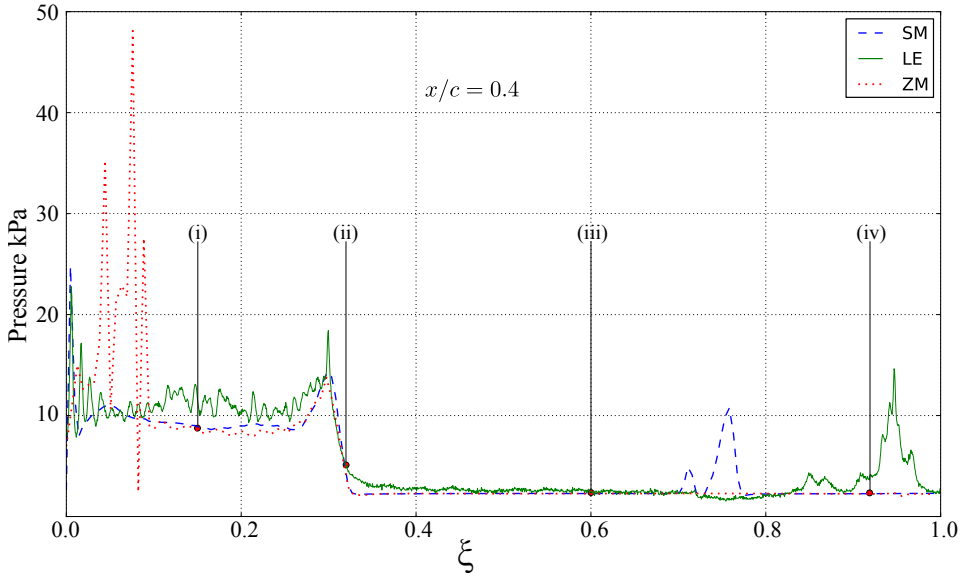

Figure 4. Pressure fluctuation vs. dimensionless time at position $x/c = 0.4$.

at $\xi = 0.78$ does not match the 2D, thus showing that 3D effects are very important when the bubble cloud collapse.

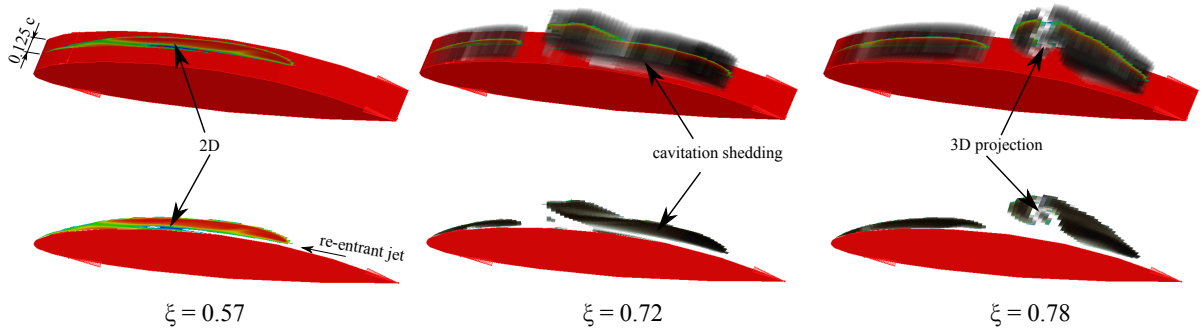

Figure 5. Analysis of Cavitation results for SM in 3D and 2D.

7. Conclusions

The study gives the following conclusions:

1. OpenFOAM and the FOSS used in the present study with the implemented math model gives credible results similar to cavitation experiments of LE. It is noted that SM results approaches more accurately than ZM ones.
2. The 3D study gives more information of cavitation shedding and cloud motion than 2D. It is necessary to understand the 3D effects in span-wise direction.

Acknowledgments

This work was financially supported by the National Natural Science Foundation of China (Project Nos. 51206087 and 51376100), and the Major National Scientific Instrument and

Equipment Development project (Grant No. 2011YQ07004901).

References

[1] Leroux J, Coutier O and Astolfi J 2005 *Physics of Fluids* **17** 052101
[2] Escaler X, Egusquiza E, Farhat M, Avellan F and Coussirat M 2006 *Mech. Syst. and Sig. Processing* **20** 983
[3] Kubota A, Kato H and Yamaguchi H 1992 *Journal of fluid Mechanics* **240** 59
[4] Coutier O, Reboud J and Delannoy Y 2003 *Intern. J. for Num. Meth. in Fluids* **42**, 527
[5] Kunz R, Boger D, Stinebring D, et al. 2000 *Computers & Fluids* **29** 849
[6] A. K. Singhal, M. M. Athavale, H. Li and Y. Jiang, 2002 *Journal of Fluids Engineering* **124**, 617
[7] Zhang X, Zhang W, Chen J, et al. 2014 *Sci. China Techn. Sci.* **57** 819
[8] Rhee S and Joshi S 2003 *Proc. ASME/JSME 4th Joint Fluids Summer Engineering Conference* pp 1157-1163
[9] Kunz R, Lindau J, et al. 2003 *Proc. Conf. on Fifth international symposium on cavitation, Osaka, Japan*
[10] Ji B, Luo X , Peng X, Zhang Y, et al. 2010 *Journal of Hydrodynamics* B **22** 753
[11] Ji B, Luo X , Wu Y, Peng X, et al. 2013 *Inter. J. of Mult. Flow* **51** 33
[12] Huang B and Wang G 2011 *Journal of Hydrodynamics* B **23** 26
[13] Ji B, Luo X, Peng X and Wu Y 2013 *Journal of Hydrodynamics* B **25** 510
[14] Morgut M, Nobile E and Bilu I 2011 *Inter. J. of Mult. Flow* **37** 620
[15] Ji B, Luo X, Wu Y and Xu H 2012 *Chinese Physics Letters* **29** 076401
[16] Hidalgo V, Luo X, et al. 2014 *Proc. of Conf. on & Nanochannels, Microchannels, and Minichannels*
[17] Negus C 2010 *Linux Bible 2010 Edition: Boot Up to Ubuntu, Fedora, KNOPPIX, Debian, openSUSE, and 13 Other Distributions* (Wiley.com) chapter 3 p 246
[18] Andersen M, Jarpner C, et al. 2011 *A interphaseChangeFoam tutorial* (Chalmers University of Technology)
[19] Franc J and Michel J 2006 *Fundamentals of cavitation* (Springer) chapter 7 pp 149-162